Chapter 2 Experimental setup

2.1 Introduction

Laser is an optical oscillator, which creates a highly directional beam of light at narrow wavelength. Figure 2.1 is the diagram of a simple laser cavity. Generally, there are three important components of lasers.

1: High reflector

2: Gain medium

3: Output coupler / partial reflector

The length L between high reflector and output coupler is the length of laser cavity. When the gain medium is excited and reaching population inversion, the light passing through the gain medium will be amplified.

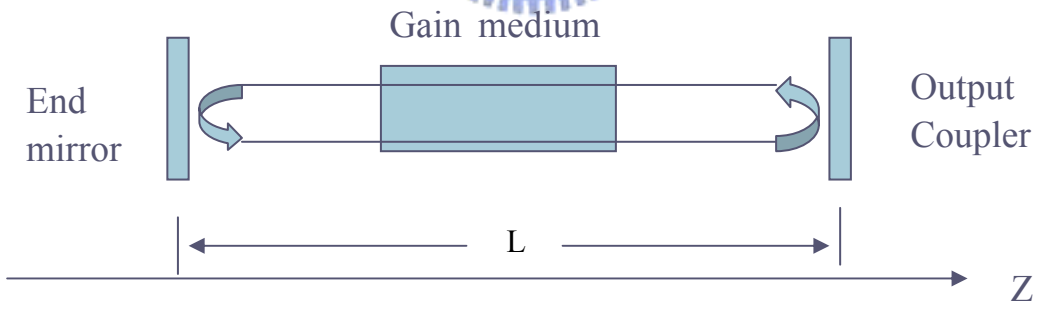

Figure 2.1: The scheme diagram of a simple laser cavity

2.2 Ultrashort pulse formation: principle of mode locking

In principle, because of the requirement of resonance condition, only the wavelengths satisfy the condition that the cavity length is the integral number of the half wavelength can survive in laser cavity, which means:

$2L = q\lambda_q$ q :any positive integral number

$$\Rightarrow \lambda_q = \frac{2L}{q},\quad \upsilon_q = \frac{C}{\lambda_q} = q\left(\frac{C}{2L}\right) \qquad C : \text{the speed of light} \tag{1}$$

and the mode space $\delta\upsilon = \frac{C}{2L}$.

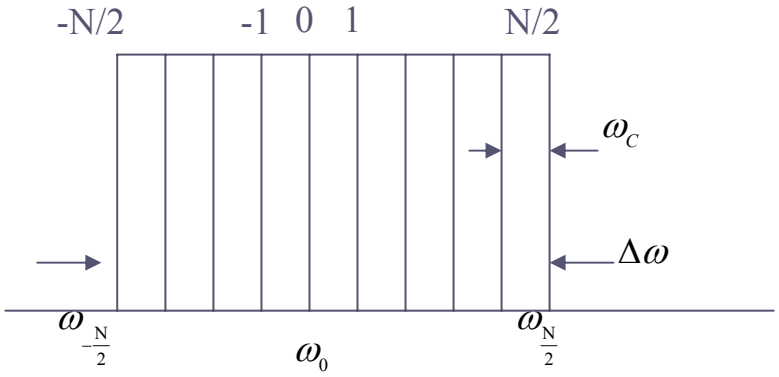

Figure 2.2: The imaginary rectangular spectra in laser cavity.

In Figure 2.2, we assume a rectangular form spectrum in laser cavity and the electric field of each cavity mode can represent as the following equation:

$$E_n(t,z) = E_0 e^{i(\omega_n t - k_n Z + \phi_n)} \tag{2}$$

In which ω, k, and ϕ denote the angular frequency, the wave vector, and the initial phase of the cavity mode, respectively. At Z=0, the superposition of all cavity modes is:

$$E(t) = E_0 \sum_{n=-\frac{N}{2}}^{n=\frac{N}{2}} e^{i(\omega_n t + \phi_n)} = E_0 \sum_{n=-\frac{N}{2}}^{n=\frac{N}{2}} e^{i[(\omega_0 + n\omega_C)t + \phi_n]} \tag{3}$$

If the initial phase of all cavity modes are the same ($\varphi_n = \varphi_0 \equiv$ constant), equation (3) can be further reduced:

$$E(t) = E_0 e^{i(\omega_0 t + \phi_0)} \sum_{n=-\frac{N}{2}}^{\frac{N}{2}} e^{in\omega_c t} \tag{4}$$

Due to $e^{i\theta} = \cos\theta + i\sin\theta$ (Euler formula), we only focus on the real number part of the equation, and equation (4) can be rearranged:

$$E(t) = E_0 e^{i(\omega_0 t+\phi_0)}(1+2\sum_{n=1}^{\frac{N}{2}}\cos n\omega_c t) = E_0\left[\frac{\sin\left(\frac{N+1}{2}\right)\omega_c t}{\sin\frac{\omega_c t}{2}}\right] * e^{i(\omega_0 t+\phi_0)} \quad (5)$$

We obtained

$$E(t) = A(t)\times e^{i(\omega_0 t+\phi_0)}, \quad A(t) = E_0\left(\frac{\sin\left(\frac{N+1}{2}\omega_c t\right)}{\sin(\frac{\omega_c t}{2})}\right) \quad (6)$$

Because the intensity of laser I(t) is proportion to $E(t)\times E^*(t)$, I(t) can be represented by equation (7):

$$I(t) \propto E(t)\times E^*(t) = A(t)^2 = {E_0}^2\left[\frac{\sin^2\left(\frac{N+1}{2}\omega_c t\right)}{\sin^2(\frac{\omega_c t}{2})}\right] \quad (7)$$

The plot of I(t) for N=4 is shown in Figure 2.3

From the above equation, I(t) would be the maximum value when $\frac{1}{2}\omega_c t = m\pi$, while the time interval between pulses $t_m = \frac{2m\pi}{\omega_c}$. Therefore, we obtained:

$$\Delta t = t_{m+1} - t_m = \frac{2\pi}{\omega_c} = \frac{1}{\delta\upsilon} = \frac{2L}{C} \quad (8)$$

The time interval between two pulses is equal to the time of pulse traveling in the laser cavity, which is called the round-trip time.

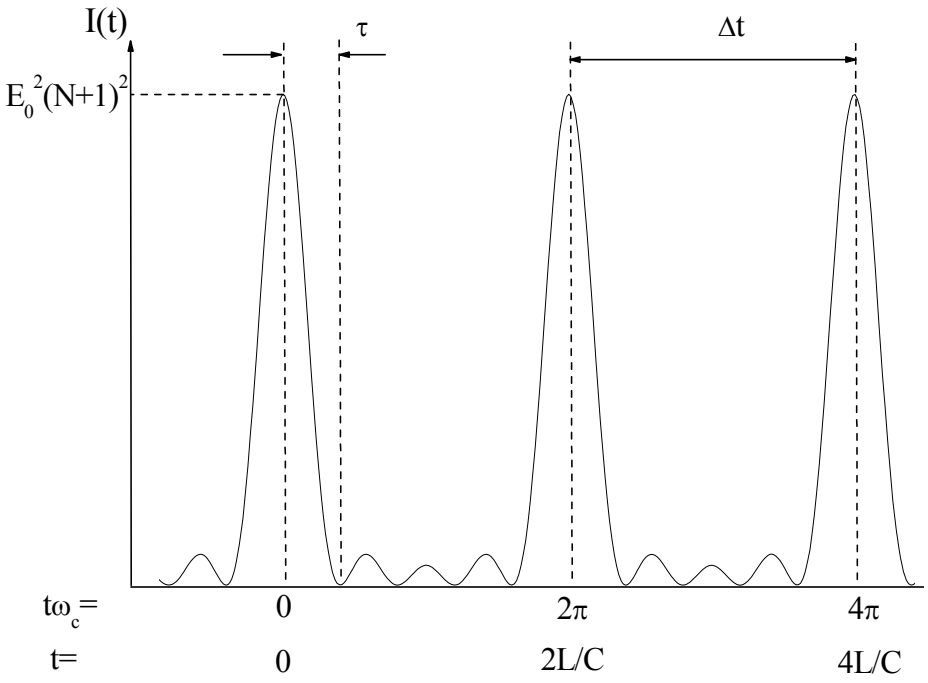

Figure 2.3: The illustration of the laser intensity change versus time for N=4.

From equation 7, the maximum intensity also can be estimated:

$$I(t)_{max} = \lim_{\frac{1}{2}\omega_c t \to 0} E_0{}^2 \frac{\sin^2\left(\frac{N+1}{2}\omega_c t\right)}{\sin^2\left(\frac{1}{2}\omega_c t\right)} \approx E_0{}^2 \frac{\left(\frac{N+1}{2}\omega_c t\right)^2}{\left(\frac{1}{2}\omega_c t\right)^2} = E_0{}^2 (N+1)^2 \qquad (9)$$

The pulse width $\tau = \frac{1}{N+1}\left(\frac{2L}{C}\right)$ (10)

The bandwidth $\Delta\nu = N\delta\nu = N\left(\frac{C}{2L}\right)$ (11)

If we multiply those two quantities, we obtained:

$$\tau\,\delta\nu = \frac{N}{N+1} \approx 1 \text{ (for } N >> 1) \qquad (12)$$

The units of τ and ν are second and Hz, respectively. The time-bandwidth product indicated that enough bandwidth is essential to produce an ultrashort pulse. For various pulse shapes, the time-bandwidth product are different (ex: for Gaussian shape pulses, $\tau\,\delta\nu = 0.441$), and only pulses that have their frequency components all

locked in phase obey this relationship. If the pulse obeys this relationship it is called a transform-limited pulse.

2.3 Active mode-locking and passive mode-locking

From the above derivation, we know that for mode-locked laser, the output will become pulsed, and the repetition rate is equal to the round-trip time, which is determined by the length of laser cavity. If we want to produce a mode-locked laser, we need to place an ultrafast shutter (the repetition rate is equal to $\frac{C}{2L}$, C: the speed of light), and the opening time must be synchronized to the mode-locked pulse. For a typical mode-locked laser, the cavity length is about 150 cm, which corresponds to ~10 ns round-trip time, and no mechanical chopper can afford this speed. Hence, a special designed mechanism is required, and there are two types of mode-locking mechanisms.

— *Active mode-locking*: this method needs an external modulation at specific frequency, and the target of the modulation can be either the gain of amplifying medium or the cavity loss.

— *Passive mode-locking*: No external modulation is required. It results from the insertion of a saturable absorber into the cavity or the optical Kerr effect of optical components, which can automatically select the mode-locked pulse.

The femtosecond Ti:sapphire laser in our laboratory is using optical Kerr effect to achieve the mode-locking condition. In normal case, the refractive index "n" of a material obeys the following relationship:

$$n = n_0 + \frac{1}{2} n_2 I \qquad (13)$$

In which, n_0 is the intrinsic refractive index of material, n_2 (positive) is the nonlinear coefficient of the refractive index, and I is the intensity of the laser. In general, n_2 is a very small value, and the second term can be ignored. However, if the intensity is high enough and the alternation caused by n_2 cannot be ignored, this effect is called optical Kerr effect.

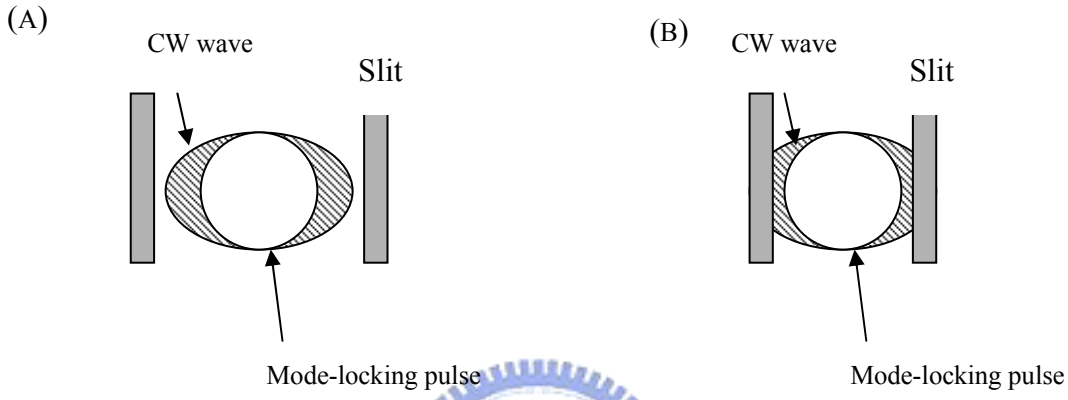

Figure 2.4: The scheme diagram for cross-sectional view of CW wave and a mode-locked pulse. (A) Slit is open; the loss of a CW wave and a mode-locked pulse is the same. (B) Slit is closed; the loss of a CW wave increases, and only the mode-locked pulse can survive

For TEM00 mode, the intensity distribution is bell shape (Gaussian) across the laser beam. Since the beam is less intense at its edge, the refractive index at the center will larger than at the edge. This causes the light to bend toward the center, and functions like a lens. In Figure 2.4A, the optical Kerr effect is more significant for mode-locked pulse than for continue wave because of its high intensity. If we place a slit, and the width is properly adjusted (Figure 2.4 B), the cavity loss of the continue wave will increase, and only the mode-locked pulse can survive and amplify in laser cavity.

2.4 Birefringent filter

For mode-locked Ti:sapphire laser, another important issue is the wavelength tuning element. In our system, the wavelength tuning is achieved by using birefringent filter, and the principle will be introduced in this paragraph.

The light enters the crystal at an arbitrary angle can be break up into two separate components that perpendicular to each other. The component on the plane, which containing the propagation direction ($\vec{k}$) and the optical axis ($\overrightarrow{OA}$), is called the extraordinary wave (e-ray). Another component, which is perpendicular to the e-ray, is called the ordinary wave (o-ray). In principle, the refractive index of o-ray (n_o) is a constant, and the refractive index of e-ray (n_e) changes with the angle between the direction of light propagate ($\vec{k}$) and the optical axis of the crystal ($\overrightarrow{OA}$). Because e-ray and o-ray have different refractive index and travel at different speed of light in the crystal, the phase shift ($\Delta\phi$) induced by this optical anisotropy effect can be calculated:

$$\Delta\phi = \frac{2\pi}{\lambda}(n_e - n_o)d \tag{14}$$

In which, d is the thickness of crystal. Only when the phase is equal to $2m\pi$ (m is an integral), the wave can survive. Therefore, we obtained:

$$2m\pi = \frac{2\pi}{\lambda}(n_e - n_o)d$$

$$\lambda = \frac{(n_e - n_o)d}{m} \tag{15}$$

Since n_e changes with the angle between $\vec{k}$ and $\overrightarrow{OA}$, the wavelength tuning can be achieved by rotating the birefringent filter.

2.5 Femtosecond Ti:sapphire laser: Mira 900-D

The femtosecond light source used in our lab is Coherent Mira Model 900-D laser. (Coherent, Inc.) Mira 900-D uses Ti:sapphire as the gain medium and is tunable from 700 to 1000 nm. The oscillator is pumped by a solid state diode-pumped frequency-doubled Nd:YVO_4 laser (Verdi^{TM} V-10, Coherent), which the output wavelength is 532 nm and the averaged power is 10 W. The optical path of the oscillator is shown in Figure 2.5. Pumping beam is focused on Ti:sapphire crystal by lens L1. M7 is the flat end mirror and M1 serves as the output coupler of laser cavity. Two prisms BP1 and BP2 are used to compensate the group velocity dispersion of the femtosecond pulse. A birefringent filter selects the wavelength of the laser output. By using optical Kerr effect, the laser cavity has been designed so that the diameter of the mode locked beam is slightly small than the non-mode locked beam. Therefore we can select the mode locked pulse with the application of a simple slit. The repetition rate is 76 MHz, and the pulse width is ~150 fs (FWHM of autocorrelation).

2.6 Autocorrelator (Mini, Inrad)

The characterization of the temporal profile of laser pulse is an important issue for time-resolved spectroscopy measurement. The response time of the electric components is limited from tens of ps (photodiode) to ps (streak camera). Therefore, for the pulse generated by the mode-locked Ti:sapphire laser, we used autocorrelation techniques to measure the pulse width. Figure. 2.6 is the optical layout of autocorrelator.

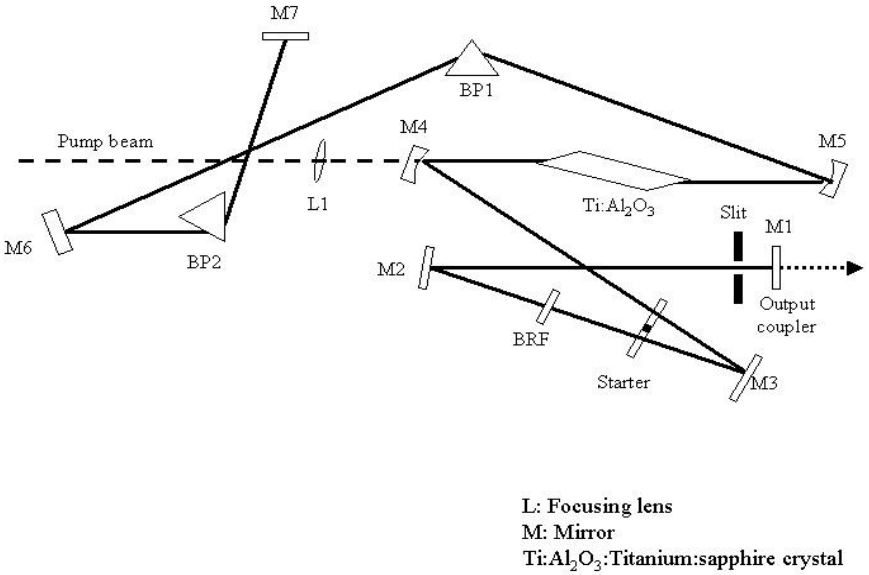

Figure 2.5: The optical scheme for Coherent Mira-900 D oscillator.

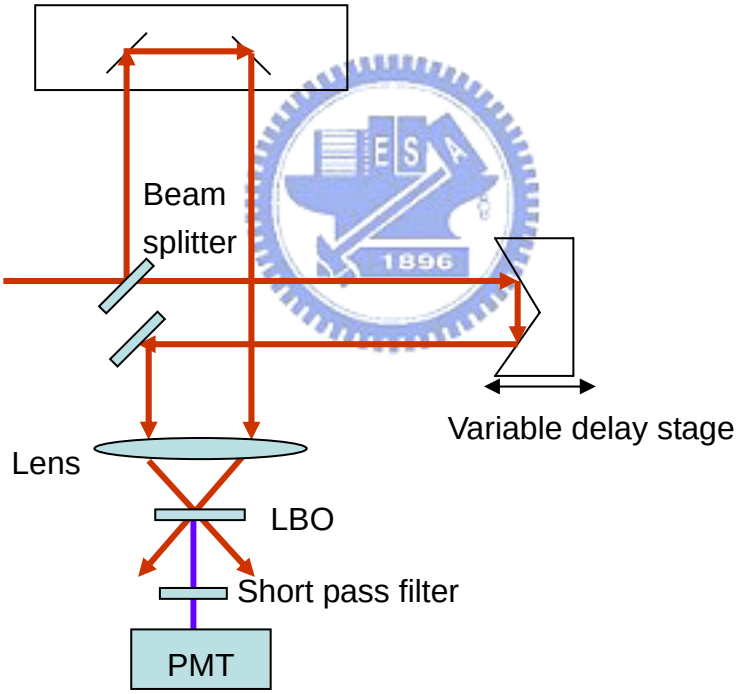

Figure 2.6: The optical layout of femtosecond autocorrelator

A beam splitter separates input pulse. The two beams are focused and overlapped on a LBO crystal. Once the delay time and the phase matching angle of those two beams are properly adjusted, the second harmonic signal will be generated and detected by PMT. The optical delay of those two beams is controlled by a

computer-controlled stage. Scanning back and forth the delay stage and monitoring the intensity change of the second harmonic signal can obtain the autocorrelation trace. For a Gaussian pulse, the FWHM of the autocorrelation trace is $\sqrt{2}$ times the FWHM of laser pulse.

2.7 Fluorescence optically gated system

Femtosecond temporally resolved spectra were obtained with an fluorescence optically gated system (FOG100, CDP) in combination with a mode locked Ti:sapphire laser (Coherent, Mira 900D). A schematic depiction is shown in Figure 2.7 The femtosecond laser system generates output pulses of duration ~150 fs (FWHM of autocorrelation) with 76 MHz repetition rate. The spectral bandwidth is 10~12 nm and the wavelength is tunable from 700 to 1000 nm. The frequency of the laser pulse is doubled by a BBO type-I crystal to generate the second harmonic signal ranging from 350~500 nm and used as excitation (pump); the residual fundamental pulse is used as a probe beam and split from the pump beam with two dichroic beam splitters (BS1, BS2). A berek polarization compensator (B) controls the polarization of the pump beam; for fluorescence lifetime measurement the relative polarization between pump and probe beams is fixed at 54.7^{o} (magic angle). The intensity of the excitation beam is properly attenuated and focused onto a rotating sample cell (S). Fluorescence is collected with two parabolic mirrors and focused onto another BBO type-I crystal (NC, thickness 0.5 mm). The gate pulse (probe) also focuses on NC for sum-frequency generation (SFG). The delay time between gate pulse and fluorescence is controlled by a stepping translational stage (maximum delay 2.0 ns, minimum step

size 6.25 fs). The SFG signal is collected by a lens (L4) and separated from the interference (pump or gate pulse) by the combination of an iris (A), a band-pass filter (F3) and a double monochromator. The signal is detected by a photomultiplier (Hamamatsu, R1527P), which is in turn connected to a computer-controlled photon-counting system.

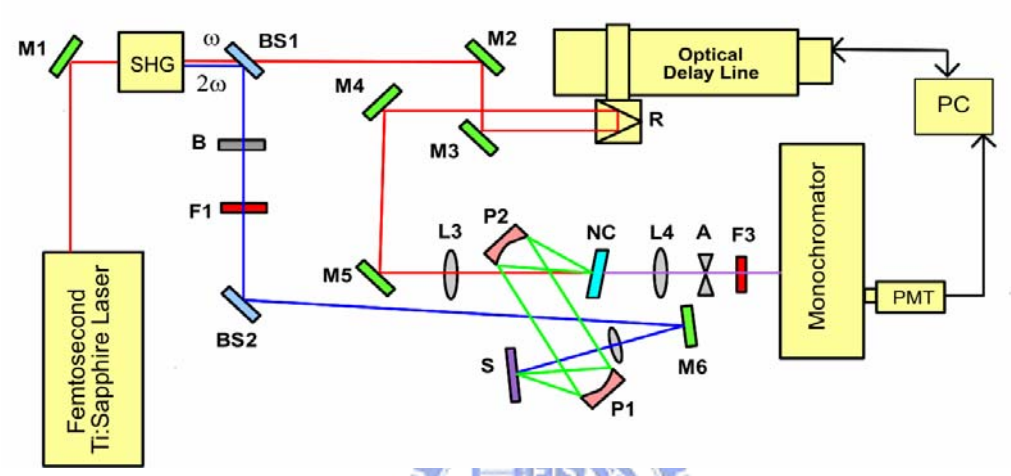

Figure 2.7 :The optical scheme for femtosecond fluorescence optical gated system. M1~M7: dielectric mirror (700~1000 nm), BS:dichroic beamsplitter, B:berck polarization compensator, P1 and P2:parabolic mirror, S: rotating sample cell.

2.8 Time-Correlated Single Photon Counting (TCSPC) system

The time-correlated single photon counting (TCSPC) system in our laboratory was purchased from PicoQuant GmbH, and the optical layout is shown in Figure 2.8. Excitation light source is introduced into the sample chamber by a reflective mirror, and an iris controls the intensity. The excitation laser is focused onto the sample holder by a focusing lens. The fluorescence is collected by high numerical aperture UV grade lens, and the distance between lens and sample cell can be adjusted by the handle ring outside the sample chamber. The collimated fluorescence then passes through an adjustable iris, and an adjustable polarizer controls the polarization. The

wavelength of the fluorescence is selected by a double subtractive monochromator (Sciencetech 9030DS). In double subtractive monochromator, the two gratings operate in a subtractive dispersion mode, which can remove the temporal and angular dispersions of the fluorescence. The silt, which locates at the center of the two monochromators, controls the spectral resolution, and the resolution is 8 nm with a 1-mm slit. Finally, the collecting signal is detected by a single photon sensitive detector (Photomultiplier, PMT), which is connected to a computer with a TCSPC-module (SPC-630, Becker and Hickl) card for data acquisition.

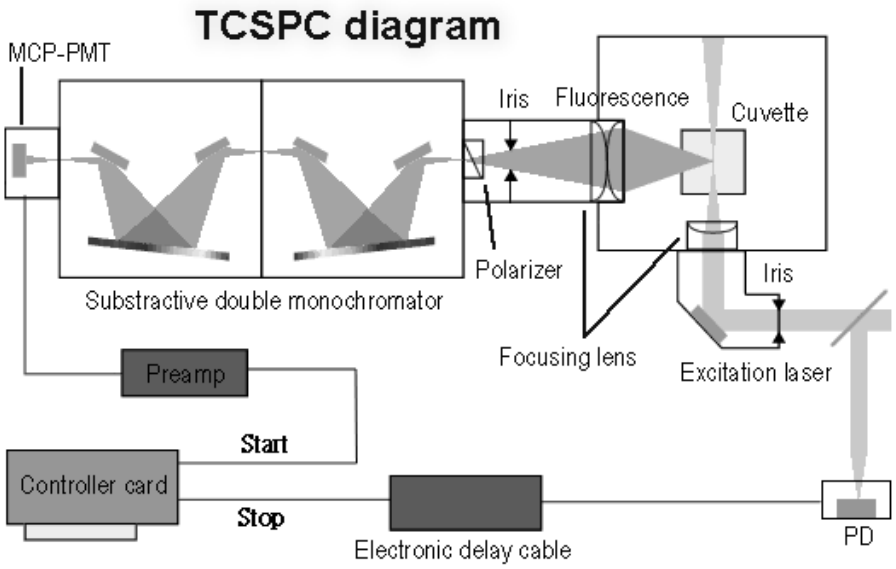

Figure 2.8: The optical layout of TCSPC system

Figure 2.9 is a scheme for the data acquisition and timing procedure of the TCSPC module. The fluorescence signal is monitored by a photon counting PMT. A constant fractional discriminator (CFD) is used to determine the exact arriving time of the photon. Simultaneously, the synchronal trigger signal of the excitation laser is sent to another CFD and used as the reference. The signal of CFD is sent to time to amplitude converter (TAC), which converts the delay time between fluorescence and the

synchronized trigger signal into voltage. The output voltage is sent to analog to digital converter (ADC) and addresses to corresponding time channel. Finally, the signal from ADC is sent to multi-channel analyzer (MCA) and the fluorescence decay is reconstructed after accumulating millions of signal. The detail description of each component will be shown in the following paragraph.

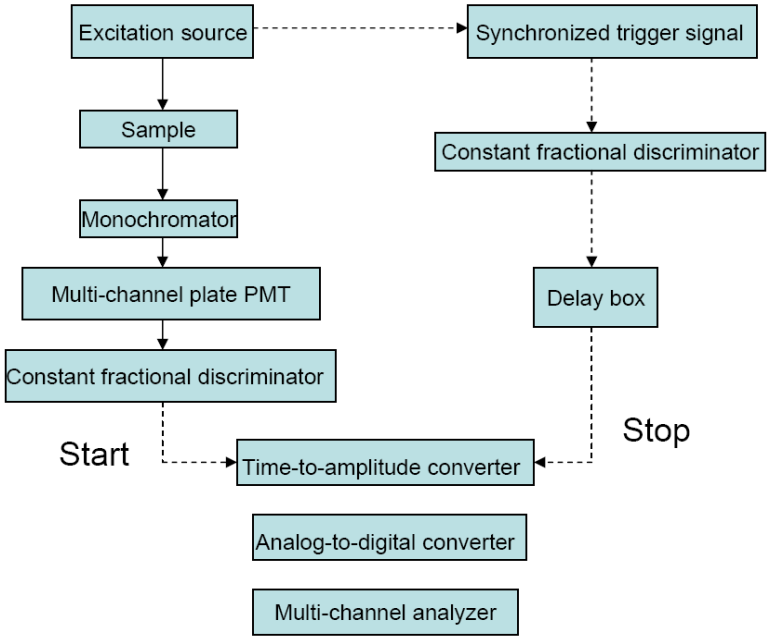

Figure 2.9: Data acquisition and timing diagram of TCSPC module

2.8.1 Double subtractive monochromator

For a monochromator used in pico or femto-second time resolved experiment, the temporal dispersion of the light with different wavelengths is not able to neglect anymore. To solve this problem, a double subtractive monochromator (Sciencetech Model 9030) was used to compensate the temporal dispersion. The first monochromator is used to select a band pass, and the variation of the optical path in different wavelength lights is removed by second monochromator. The spectral

dispersion is selected by using interchangeable slits with 0.5, 1.0, 2.0 mm, and the corresponding spectral resolution is 4, 8, and 16 nm, respectively.

2.8.2 Constant fractional discriminator (CFD)

Constant fractional discriminator is used to determine the arriving time of photon and synchronized signal. Figure 2.10 is the illustration of the principle of CFD; a part of input pulse is inverted and delayed with constant delay time. The sum of input pulse and inverted pulse generates a zero-crossing point as we can see in Figure 2.10. Since the temporal position of the crossover point is independent of the pulse amplitude, the time jitter caused by the amplitude fluctuation of the detector pulses can be eliminated by this method. On the other word, the CFD also contains a window discriminator which can reject the signal smaller or outside of the selected amplitude interval. By adjusting this interval, the noise from the environment can be effectively rejected.

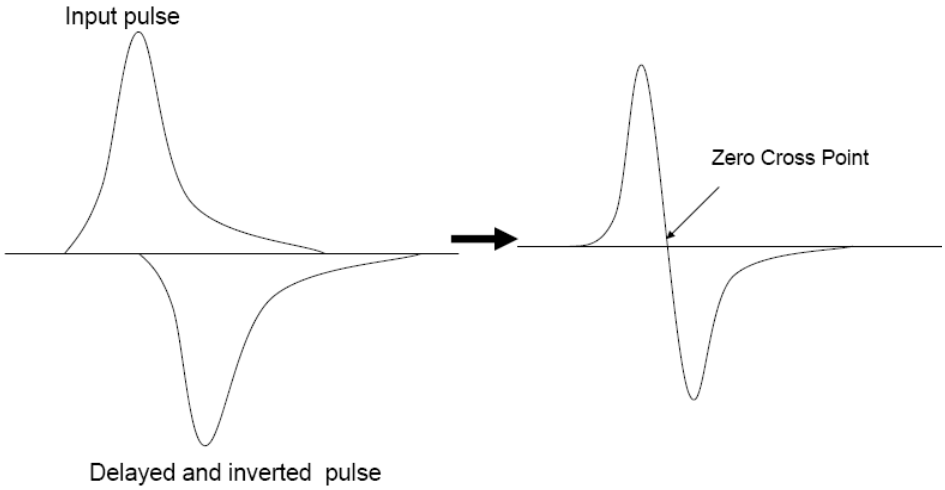

Figure 2.10: Basic function of CFD, a small portion of the input signal is inverted, and the arriving time is determined by the zero cross point.

2.8.3 Time-to-amplitude converter (TAC)

The time-to-amplitude converter is used to determine the delay time between detected photon and sync signal. When TAC receives the fluorescence pulse signal form CFD, it generates a linear ramping voltage and stop by the sync pulse train. The output voltage of TAC depends linearly on the time interval between photon and sync pulse. In contrast to tradition start-stop method, which starts from a sync pulse and stops at the fluorescence signal, this ‘reversed start-stop‘ method reduces the speed requirements of TAC, because its working cycle is performed with the photon detection rate instead of the considerable higher pulse repetition rate.

If the fluorescence intensity is too high, more than one photon will come to TAC within one excitation period. At this time, TAC starts to charge as the first photon arrives, and the second photon is neglected. Because only the first arriving photon is counted, the fluorescence lifetime obtained in this condition is shorter than the actual value, and this phenomenon is called “multi-photons pile up”. To avoid the pile up, the repetition rate of the detected photon is controlled lower than 1/100 of the repetition rate of excitation source.

2.8.4 Analog-to-digital converter (ADC)

The analog-to-digital converter converts TAC signal into the address of the memory. The ADC must have very high accuracy; because it has to resolve TAC signals into 4096 time channels, and the width of particular channel is only ~0.024% of the total voltage amplitude.

2.8.5 Multi-channel analyzer (MCA)

After the output voltage of TAC converts into the address of the memory, the data are saved in memory. After accumulating billions of photons, the fluorescence decay is reconstructed.

2.8.6 Variable delay box

The variable delay box is composed of coaxial cables, and no power is required to operate this component. The main purpose of this box is to delay the SYNC pulses so that they reach the TAC after the start pulse within the selected time range of interest. It provides a variable delay input signal from 0~63 ns.

2.8.7 Microchannel-plate photomultiplier Tube (MCP PMT)

MCP PMT includes anode (generates the photoelectron), microchannel plate (formed by capillary), and the cathode (receives the amplified photoelectron). When a high voltage is applied in anode and cathode, the photoelectron emitted from the anode will be collected and send into the capillary. The diameter of capillary is about 10 μm, and one layer of amplification media is coated on the inside wall of capillary. The cathode detects the amplified signal. Because this single photon detector is highly sensitive, and even dimmed ambient light can permanently damage it, there is a built-in shutter that interlocked with the chamber lid to prevent any damage caused by accident.